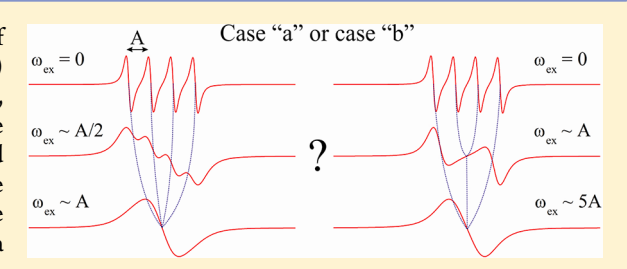


Single Crystal EPR of the Mixed-Ligand Complex of Copper(II) with L-Glutamic Acid and 1,10-Phenanthroline: A Study on the Narrowing of the Hyperfine Structure by Exchange

Nicolás I. Neuman, Vanina G. Franco, Felix M. Ferroni, Ricardo Baggio, Mario C. G. Passeggi, Alberto C. Rizzi, and Carlos D. Brondino

Supporting Information

ABSTRACT: We report an EPR study at X- and Q-bands of polycrystalline and single crystal samples of the mixed copper(II) complex with L-glutamic acid (glu) and 1,10-phenantroline (phen), $[Cu(glu)(phen)(H_2O)]^+ NO_3^- \cdot 2(H_2O)$. The polycrystalline sample spectrum at Q-band showed well resolved g_{\parallel} and g_{\perp} features and partially solved hyperfine structure at g_{\parallel} , typical for weakly exchange coupled systems. This is confirmed from the angular variation of the EPR spectra which shows for certain magnetic field orientations a partially solved hyperfine structure characteristic of weak exchange,



whereas a single Lorentzian line corresponding to strong exchange is observed for others. Analysis and simulation of the single crystal EPR spectra were performed using the random frequency modulation model of Anderson. Numerical simulations of the angular variation of the EPR spectra showed that the narrowing of the hyperfine structure is due to an exchange-mediated mechanism in which transitions between any pair of lines are equally likely. The exchange interaction responsible for this process is mediated by hydrophobic interactions between two phen molecules and a mixed chemical path of the type CuA-O_{an}H···O-C-O_{eq}-CuB, for which we evaluated an average isotropic exchange parameter $|J| \approx 25 \times 10^{-4}$ cm⁻¹.

■ INTRODUCTION

The magnetic characterization of paramagnetic systems coupled by isotropic exchange interactions mediated by noncovalent bonds constitutes a research subject with applications in distinct areas such as supramolecular chemistry¹⁻³ and biological chemistry.⁴⁻⁶ Exchange interactions transmitted by these chemical paths are too small $(I < 0.1 \text{ cm}^{-1})$ to be precisely evaluated by conventional bulk magnetic measurements,³ but they can be accurately and selectively measured by electron paramagnetic resonance (EPR).^{7,8} These systems may show EPR properties associated with two well-differentiated regions, one reminiscent of that corresponding to magnetically isolated paramagnetic centers in which the exchange interaction produces a broadening of the resonance lines of the order of the exchange frequency $\omega_{\rm ex}$ (weak exchange), and the other corresponding to a single exchange-narrowed resonance line (strong exchange). The transition between these two states was theoretically analyzed by Anderson using the so-called random frequency modulation model for the case of extended systems formed by two different $S = \frac{1}{2}$ spins coupled by Heisenberg exchange interaction $(H_{\rm ex} = -JS_1 \cdot S_2, \, \omega_{\rm ex} \approx J/\hbar)$, and later used by Farach et al. to explain the narrowing of the hyperfine structure in systems having nuclear spin values $I = \frac{1}{2} I_2$ to $^{5}/_{2}$. An alternative approach to analyze the S = 1/2 case was

also performed on the basis of generalized Bloch equations. 12 Anderson's model can also be applied to analyze the motional narrowing experienced by paramagnetic species in solution, where ω_{ex} is associated with the rate of the local Brownian

Anderson's theory has been successfully verified for systems showing two resonance lines in the absence of exchange, as is the case of compounds formed by two magnetically nonequivalent copper ions and of dimeric systems using single crystal EPR spectroscopy. ^{13,14} The solution in these cases is unique, allowing one to evaluate spectral modifications in situations of weak ($\omega_{\rm ex} < g\beta\Delta B/2\hbar$), intermediate ($\omega_{\rm ex} \approx$ $g\beta\Delta B/2\hbar$), and strong exchange ($\omega_{\rm ex} > g\beta\Delta B/2\hbar$), with ΔB being the separation between the two resonance lines. In contrast, the application of Anderson's theory to systems with nuclear spins $I \ge 1$ requires that at least two extreme cases must be taken into account. One of them, case "a", implies that exchange couples equally each line of the 2I + 1 hyperfine structure (HFS) components to all other lines of the spectrum, whereas in the other, case "b", the transitions occur with equal

September 3, 2012 Received: Revised: November 22, 2012 Published: November 27, 2012

[†]Departamento de Física, Facultad de Bioquímica y Ciencias Biológicas, Universidad Nacional del Litoral, Ciudad Universitaria, Paraje El Pozo, S3000ZAA Santa Fe, Argentina

[‡]Gerencia de Investigación y Aplicaciones, Comisión Nacional de Energía Atómica, Avenida Gral Paz y Constituyentes, San Martín, Buenos Aires, Argentina

probability only between adjacent lines. The elucidation of which mechanism narrows the hyperfine structure, which is virtually unstudied to date, is essential for a reliable determination of the *J*-value, and constitutes the object of our paper.

Copper-glutamate and copper-aspartate complexes and their adducts with aromatic amines are appropriate systems to apply Anderson's theory in situation of strong, intermediate, and weak exchange. 13,15,16 In the solid state, the copper complexes with aspartic and glutamic acids give rise to polymeric compounds of the type -Cu-aa-Cu-aa-Cu-, where each copper atom is coordinated in a bidentate fashion by the amino acid (aa) function from one amino acid molecule, and the side chain carboxylate from another amino acid molecule. 17,18 This configuration is either modified or even disrupted in the mixed copper complexes with aromatic amines where the amines not only coordinate the metal ions but also interact through π – π interactions, which originates compounds with rather different structural properties. 19-24 An additional consequence of the π - π interactions is the formation and stabilization of cocrystals of the coordination complexes. 19,24 A common structural feature of these compounds with relevance in magnetism is that noncovalent bonds such as hydrogen bridges and aromatic ring stacking are appropriate chemical paths to transmit weak exchange interactions that can be evaluated by single crystal EPR spectroscopy. 13,14,16,25-27

We report here a single crystal EPR study at X- and Q-bands of the mixed copper(II) complex with L-glutamic acid (glu) and 1,10-phenantroline (phen), [Cu(glu)(phen)(H₂O)]⁺NO₃⁻ 0.2-(H₂O), hereafter Cu(glu)phen. The angular variation of the EPR spectra shows for certain magnetic field orientations a partially solved hyperfine structure typical of weak exchange, whereas a single Lorentzian line corresponding to strong exchange is observed for others. With the objet explained above, we analyze the transition between these two situations under the assumption of the random frequency modulation model.

EXPERIMENTAL METHODS

All chemicals of commercially available reagent grade were used as received. Single crystals of Cu(glu)phen were obtained as previously reported with some modifications. ²⁴ Copper nitrate trihydrate (Fluka, 0.24 g (1 mmol)), L-glutamic acid (Sigma, 0.226 g (1.5 mmol)) and 1,10-phenanthroline (Sigma-Aldrich, 0.198 g (1 mmol)) were added to 20 mL of deionized water. The mixture was stirred for a few minutes at room temperature, and the pH was adjusted to 2.5 with 0.1 M NaOH; the solution was filtered through a cellulose acetate membrane (pore size 0.2 μ m) and left to crystallize at room temperature. After a week, elongated prismatic blue crystals were obtained and separated by filtration, washed with cold water, and stored in a dry environment.

Since distinct reports on the synthesis of mixed copper complexes with aspartic and glutamic acid with aromatic amines showed different structures despite using identical procedures, and as the synthesis of Cu(glu)phen was performed with a procedure different to that previously reported, elemental analysis and X-ray diffraction (XRD) were performed to verify the structure of the compound synthesized here. Single-crystal XRD data were collected on a Bruker Smart CCD area detector using Mo K α radiation (λ = 0.71073 Å). The structure was solved by direct methods (SHELXS-97) and refined by full-matrix least-squares on F2 (SHELXL-97).

Hydrogen atoms relevant for the description of the H-bonding (O–H's and N–H's) were found in a late difference Fourier synthesis and further idealized; those attached to carbon were positioned theoretically. In all cases, H atoms were allowed to ride during refinement, with $U_{\rm iso}({\rm H})=1.2/1.5U_{\rm eq}({\rm Host})$. A complete set of the results of the XRD crystallographic structural data has been deposited at the Cambridge Structural Database (CSD) in CIF format (deposition number CCDC 891324). Details on the data collection procedures, structural determination methods, and structure refinement are given as Supporting Information. These data together with elemental analysis confirmed that the crystal structure of the compound obtained by us corresponds to that reported by Biswas et al. 24

X-band and Q-band CW EPR spectra were recorded at room temperature on powder and oriented single crystal samples on a Bruker EMX plus spectrometer, with 100 kHz field modulation. Powder samples were obtained by grinding single crystals. Variable temperature EPR measurements at X-band were also performed on powder samples in the range 100 K-room temperature.

The morphology of the single crystals, necessary to orient the sample for the single crystal EPR experiment, was determined by measuring the angles between crystal faces using a Carl Zeiss Axiolab goniometric microscope. The triclinic crystals are elongated prisms which grow along the a axis and show well-defined (001), (010), and (011) crystal faces. A (010) face was glued to a KCl cubic crystal, in order to record EPR spectra in the ab^* , c^*a , and c^*b^* crystalline planes ($b^* = c \times a$; $c^* = a \times b^*$). The angular variation of the EPR spectra was obtained as explained elsewhere. The central position of each spectrum was obtained by least-squares fitting the field derivative of one, two, or four Lorentzian functions to the spectra. EPR spectra were analyzed with the EasySpin toolbox and homemade programs based on MATLAB.

■ RESULTS AND DISCUSSION

Crystal and Molecular Structure. A brief description of the crystal structure is presented in order to interpret the EPR experiment. Cu(glu)phen consists of two independent [Cu- $(glu)(phen)(H_2O)^{-1}NO_3^{-1}\cdot 2(H_2O)$ units crystallizing in the triclinic space group P1 identified as CuA and CuB in Figure 1A (both nitrate and uncoordinated water molecules were omitted for clarity). These units are very similar, with both Cu-N₃O₂ copper coordination polyhedra plus their phenanthroline groups being almost centrosymmetrically related around (0.5, 0.5, 0.5) (mean/maximum deviation from the -1 symmetry: 0.08 Å/0.20 Å). Deviations from a true -1symmetry are thus mainly restricted to the glutamate groups (Figure 1B). The coordination around the copper(II) ion is nearly square pyramidal with two N atoms from a phen ligand and one O and one N from a glutamate anion, all as equatorial ligands, and one oxygen from a water molecule in apical position (Figure 1A). Since the glutamate ions are singly protonated, the main molecule ends up bearing a +1 charge, which is balanced by the external NO₃⁻ counterion. Two hydration water molecules per copper cation complete the formula (see Supporting Information for more details).

The crystal structure of Cu(glu)phen is stabilized by hydrophobic interactions between phen molecules coordinated to CuA and CuB atoms belonging to different unit cells ($d_{\text{CuA}-\text{CuB}'}$, 6.6563(5) Å and $d_{\text{CuA}-\text{CuB}''}$, 8.8225(5) Å, see Figure 2B), which defines chains of Cu(glu)phen molecules running along the a axis. The closest neighboring chains interact

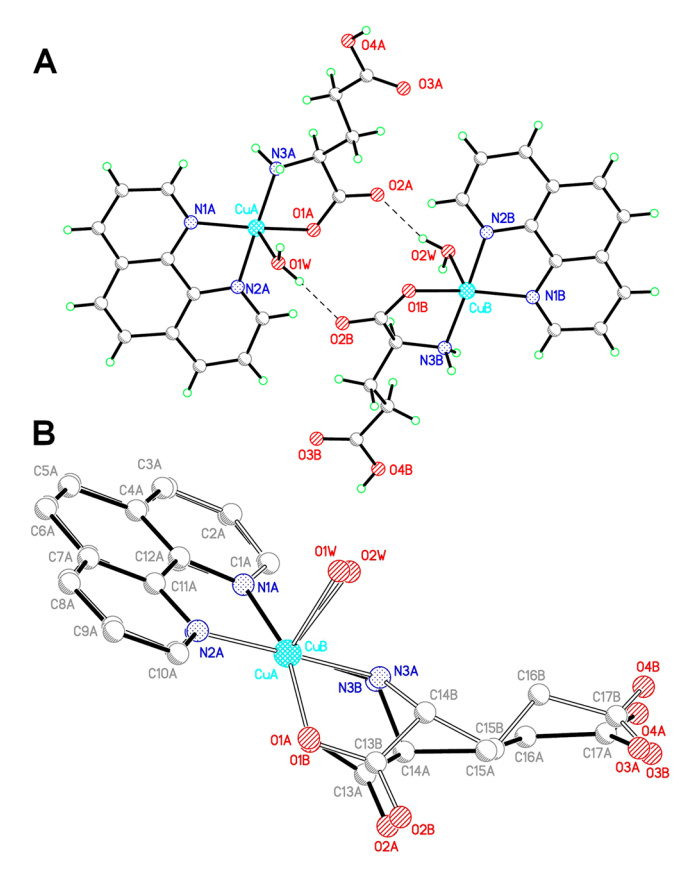


Figure 1. (A) Coordination around the two crystallographically independent copper centers of Cu(glu)phen. (B) Molecular overlap of both A and B moieties (full and empty lines, respectively) through a 1-x, 1-y, 1-z pseudo operation, showing compliances and departures from a real -1 symmetry.

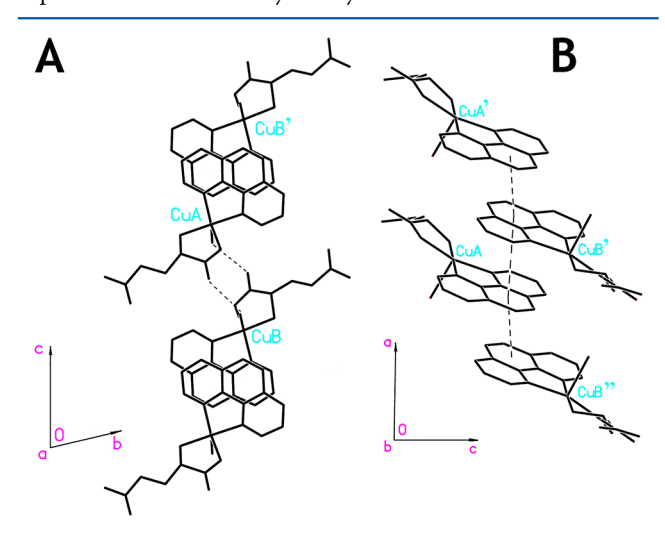


Figure 2. $\pi - \pi$ interactions in Cu(glu)phen. (A) View down the *a* axis of two chains of Cu(glu)phen molecules. Dashed lines represent the CuA $-O_{ap}H\cdots O-C-O-CuB$ path shown in Figure 1A. (B) View down the *b* axis of a single chain. Dashed lines indicate the CgA...CgB intercentroid distances (3.847(3), 4.142(3)Å) between quasi parallel phenyl groups (dihedral angle: 1.7(1)°). CuA and CuB atoms belong to the same unit cell whereas CuA', CuB', and CuB" identify copper atoms from adjacent unit cells. Symmetry codes: (single prime) *x*, *y*, 1 + *z*; (double prime) -1 + x, y, 1 + z.

through a mixed chemical path of the type CuA $-O_{ap}H\cdots O-C-O_{eq}-CuB$ ($d_{CuA-CuB}$, 6.6101(5) Å) that involves Cu ions

belonging to the same unit cell (Figures 1A and 2A). The structure is also stabilized by a complex network of strong hydrogen bonds that involves neighboring copper ion chains and nitrate molecules (see Supporting Information for details).

EPR Measurements. The X-band and Q-band EPR spectra of a polycrystalline sample of Cu(glu)phen at 298 K are shown in Figure 3. No significant differences were observed at low

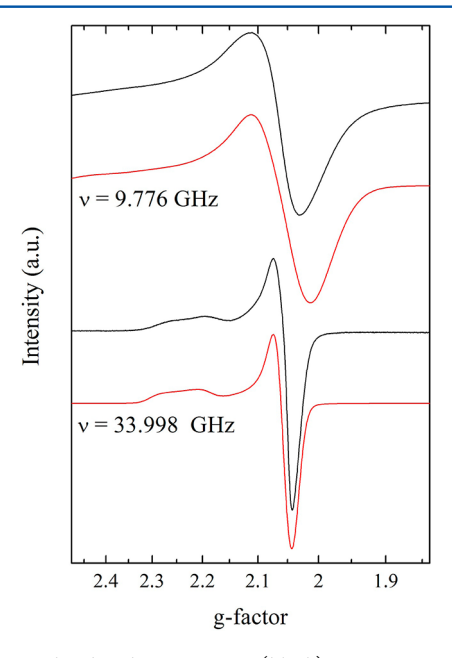


Figure 3. X- and Q-band EPR spectra (black) at room temperature of polycrystalline samples of Cu(glu)phen together with simulation (red). The g-values used in the simulation were those of the single crystal EPR experiment (Table 1) and the A_{\parallel} -value was 175×10^{-4} cm⁻¹. The anisotropic linewidths were LW₁ = 19 mT, LW₂ = 14 mT and LW₃ = 7 mT for X-band and LW₁ = 22 mT, LW₂ = 14 mT and LW₃ = 7 mT for Q-band.

temperatures (see Supporting Information). The X-band spectrum shows a single asymmetric line at $g \sim 2.07$, whereas the Q-band spectrum is nearly axial with partially solved hyperfine structure in the g_{\parallel} -region. Simulation of these spectra was performed assuming a Hamiltonian consisting of a Zeeman term and hyperfine interaction with the copper nucleus, in which the g-values were obtained from the single crystal EPR experiment (see below).

Figure 4 (left panels) shows representative single-crystal EPR spectra obtained in the c*a crystal plane at X- and Q-band and room temperature. A single Lorentzian-shaped resonance line, characteristic of strong exchange, was observed for some magnetic field orientations at both microwave frequencies (see e.g. spectra at 0° and 140°). In contrast, spectra with partially solved hyperfine structure, typical of weak exchange, were obtained for field orientations in the range of 20° to 120°. Note that this range corresponds to a field orientation region around g_{||} indicating that g-and A-tensors are coaxial as expected for copper(II) centers in square planar coordination. Spectra with similar features were observed in the ab^* and c^*b^* planes (see Supporting Information). The comparison of the spectra at both bands indicates that CuA and CuB sites show the same gand A-values, as no significant differences were detected (Figure 4). This is in line with the pseudo inversion center of Cu(glu)phen (Figure 1B), which implies that the crystallo-

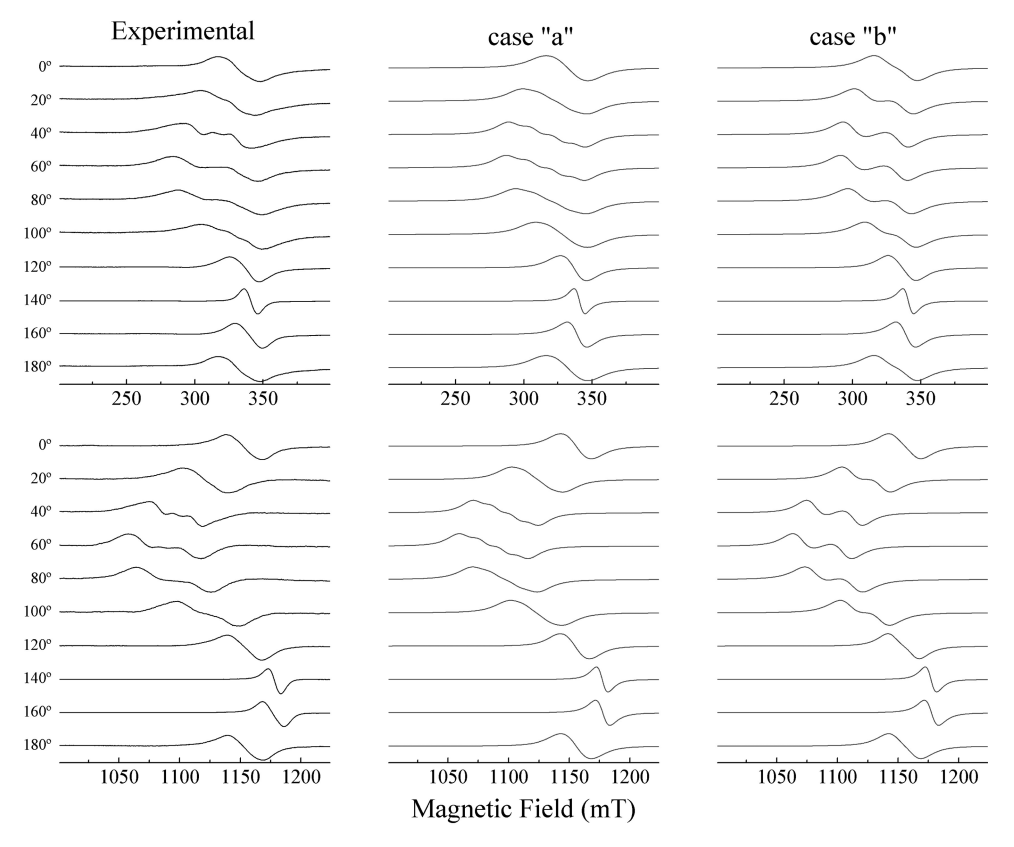


Figure 4. Experimental EPR signals of Cu(glu)phen in the c^*a crystal plane (left panel) together with simulation for cases "a" and "b" (center and right panel, respectively). The top and bottom panels correspond to the spectra at X- and Q-band, respectively. The magnetic field orientation relative to the ab^*c^* crystal frame is indicated. The spin Hamiltonian parameters for simulation were the g-tensors given in Table 1, $A_{\parallel}=182\times10^{-4}$ cm⁻¹ and $A_{\perp}=19\times10^{-4}$ cm⁻¹). The exchange frequencies ($\omega_{\rm ex}$) were $\hbar\omega_{\rm ex}=74\times10^{-4}$ cm⁻¹ and 370×10^{-4} cm⁻¹ for case "a" and case "b", respectively. The linewidths were evaluated from the second moment of the dipolar interaction (see Supporting Information) plus a constant intrinsic line width of 2 mT. g- and A-tensors were assumed to be coaxial, as deduced from the angular variation of the experimental spectra.

graphically independent CuA and CuB centers are indistinguishable by EPR under these experimental conditions.

Single crystal EPR and polycrystalline sample spectrum at Q-band, which showed well resolved g_{\parallel} and g_{\perp} features together with partially solved HFS at g_{\parallel} , indicate that Cu(glu)phen is a weakly exchange coupled system.

The Spin Hamiltonian and the Molecular g-Tensor of the Cu(II) lon. The spin Hamiltonian for Cu(glu)phen corresponds to that of an extended system with two magnetically equivalent S = 1/2 centers with nuclear spin I = 3/2 coupled by exchange interaction and is given by

$$\hat{\mathcal{H}} = \beta(\mathbf{S}_A + \mathbf{S}_B) \cdot \mathbf{g} \cdot \mathbf{B} + \mathbf{S}_A \cdot \mathbf{A} \cdot \mathbf{I}_A + \mathbf{S}_B \cdot \mathbf{A} \cdot \mathbf{I}_B - J_{AB} \mathbf{S}_A \cdot \mathbf{S}_B$$
$$-J_{AB'} \mathbf{S}_A \cdot \mathbf{S}_{B'} - J_{AB''} \mathbf{S}_A \cdot \mathbf{S}_{B''}$$
(1)

where **g** is the molecular **g**-tensor of the copper sites, **A** is the hyperfine tensor, and $J_{AB'}$, $J_{AB'}$, and $J_{AB''}$ are the isotropic exchange parameters between copper A and the nearest B, B', and B'' neighbors (see Figure 2), while the other symbols have the usual meaning. Note that indexes A and B can be exchanged to account equivalently for interactions between a center B and its A, A' and A'' neighbors. These exchange terms as well as the sum over all unit cells in eq 1 were omitted for simplicity. The Zeeman term in eq 1 determines the central position (gravity center) of the overlapped resonance lines of both copper centers, and the following two terms account for the hyperfine structure. The exchange terms produce the shift/merging of all spectral lines toward/at the gravity center of the spectrum,

depending on the orientation of the magnetic field. As the exchange interaction commutes with the Zeeman term, the gravity center of the spectra at X- and Q-bands is not affected by exchange. In contrast, the exchange Hamiltonian does not commute with the hyperfine term, what produces the narrowing effect. As both hyperfine and exchange interactions are microwave frequency independent, no significant differences would be expected at X- and Q-bands regarding the collapse phenomenon, as shown in Figure 4. Interactions such as anisotropic dipole—dipole interactions, anisotropic exchange and superhyperfine coupling with the N nuclei are omitted in eq 1 as these interactions in absence of exchange yield mainly broadening of each hyperfine component without modifying significantly its position. If the exchange interaction is much lower than all interactions that produce broadening (weak exchange), the spectra should consist of four superimposed Gaussian-shaped hyperfine components. In contrast, a single exchange-collapsed Lorentzian resonance line should be observed in situations of strong exchange. The latter is observed for magnetic field orientations around 0 and 140° (Figure 4).

Figure 5 shows the X-band angular variation of the g^2 -factors in the three crystal planes obtained from the gravity centers of the spectra. These data were used to obtain the molecular gtensor (eq 1) by least-squares fitting eq 2 to the data

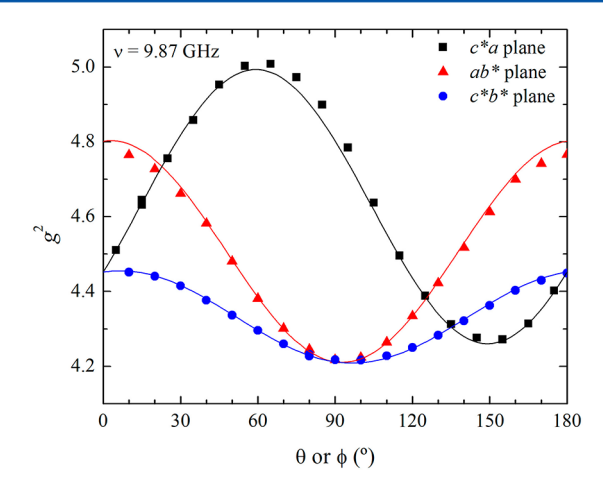


Figure 5. Angular variation of the squared *g*-factors at 9.8 GHz in three orthogonal crystalline planes of Cu(glu)phen. The solid lines were obtained with the parameters included in Table 1.

$$g^{2}(\theta, \varphi) = g_{xx}^{2} \sin^{2}\theta \cos^{2}\varphi + g_{yy}^{2} \sin^{2}\theta \sin^{2}\varphi + g_{zz}^{2}$$
$$\cos^{2}\theta + 2g_{xy}^{2} \sin^{2}\theta \cos\varphi \sin\varphi + 2g_{zx}^{2}$$
$$\sin\theta \cos\varphi \cos\theta + 2g_{zy}^{2} \sin\theta \sin\varphi \cos\theta$$
(2)

Similar results were obtained at Q-band (Supporting Information). The components of the **g**-tensor obtained at both bands together with its eigenvalues and eigenvectors are given in Table 1.

Table 1. Values of the Components of the g²-Tensor (Eq 1) Obtained by Least-Squares Analysis at both Microwave Frequencies^a

9.87 GHz	34.0 GHz
$g_{xx}^2 = 4.802(4) g_{xy}^2 = 0.029(5)$	$g_{xx}^2 = 4.817(4) g_{xy}^2 = 0.101(5)$
$g_{yy}^2 = 4.212(4) g_{zx}^2 = 0.322(5)$	$g_{yy}^2 = 4.186(4) g_{zx}^2 = 0.344(5)$
$g_{zz}^{2} = 4.451(4) g_{zy}^{2} = 0.028(5)$	$g_{zz}^2 = 4.449(4) g_{zy}^2 = 0.046(5)$
$g_1 = 2.235(3)$	$g_1 = 2.244(3)$
$g_2 = 2.052(2)$	$g_2 = 2.042(2)$
$g_3 = 2.064(2)$	$g_3 = 2.060(3)$
$\mathbf{a}_1 = [0.858(2), 0.050(6), 0.511(4)]$	$\mathbf{a}_1 = [0.852(2), 0.129(5), 0.508(3)]$
$\mathbf{a}_2 = [0.045(4), 0.98(2), -0.17(7)]$	$\mathbf{a}_2 = [-0.20(3), 0.977(9), 0.081(5)]$
$\mathbf{a}_3 = [-0.511(5), 0.17(8), 0.84(2)]$	$\mathbf{a}_3 = [-0.49(1), -0.17(6), 0.858(5)]$

 ${}^{a}g_{1}$, g_{2} , and g_{3} , and a_{1} , a_{2} , and a_{3} are the eigenvalues and eigenvectors of \mathbf{g}^{2} in the $ab^{*}c^{*}$ coordinates system, respectively.

The g_1 direction (\mathbf{a}_1) is lying approximately along the normal (\mathbf{n}) to the plane of copper equatorial ligands (angle $\mathbf{a}_1 - \mathbf{n}_A = 3.15^{\circ}$ for CuA, angle $\mathbf{a}_1 - \mathbf{n}_B = 5.19^{\circ}$ for CuB) whereas the g_2 and g_3 directions are lying approximately between the equatorial bonds (Figure 6). The relation between the g-values, $g_1 > g_2 \approx g_3$, indicates that the main contribution to the magnetic ground state is given by the $d(x^2 - y^2)$ orbital, as expected for a copper site in approximately square pyramidal coordination. The anisotropy of g_{\perp} together with the fact that g_2 and g_3 directions are not along the bonds (angle $\mathbf{a}_2 - \mathbf{Cu}$, N1A = 25.4°, angle $\mathbf{a}_3 - \mathbf{Cu}$, N1A = 67.3°) (Figure 6), as expected for symmetry reasons for a Cu(II) ion in \sim ON₃ square planar environment, indicate that the ligand-field component acting along the ground-state orbital directions lowers the symmetry

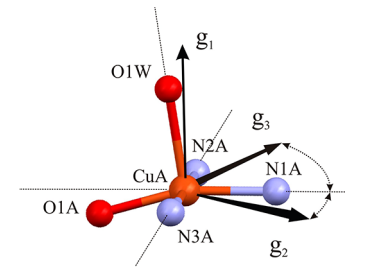


Figure 6. Principal axes (black arrows) of the g-tensor at X-band for the Cu_A site. Similar orientation was obtained from the Q-band data. The dotted line along the bonds is intended to help the eye.

producing a small admixture of mainly the $d(3z^2 - r^2)$ orbital and in a lesser extent of the d(xy), d(xz), and d(yz) excited-state orbitals into the ground state.³¹

The Exchange Frequency and its Influence on the Hyperfine Structure. Within the linear response theory, the absorption spectrum in the frequency domain observed in CW-EPR experiments is given by^{32,33}

$$\begin{split} I(\omega) &\propto \frac{\chi''}{\omega} \\ &= \frac{V}{2kT} \int_{-\infty}^{\infty} \langle M_{h_1}(t) M_{h_1} \rangle \mathrm{e}^{-i\omega t} \, \mathrm{d}t \\ &= \frac{V}{2kT} \langle M_{h_1} M_{h_1} \rangle \int_{-\infty}^{\infty} \varphi(t) \mathrm{e}^{-i\omega t} \, \mathrm{d}t \end{split} \tag{3}$$

where χ'' is the imaginary part of the dynamic susceptibility, ω is the microwave frequency, V is the volume, k is the Boltzmann constant, and T is the absolute temperature. M_{h1} is the component of the magnetization operator along the direction of the microwave magnetic field \mathbf{h}_1 , perpendicular to the applied static magnetic field \mathbf{B} , and $M_{h1}(t)$ is its time dependence. $\varphi(t)$ is called the relaxation function, and $\langle ... \rangle$ indicates a thermal average calculated over the spin system. Equation 3 relates the absorption spectrum observed in EPR experiments to the Fourier transform of $\varphi(t)$.

In the absence of exchange interactions, the EPR spectrum of an extended lattice composed by magnetically equivalent Cu(II) ions should consist of four equally strong resonance lines with positions $\omega_i + m_{\rm I}A/\hbar$, where $m_{\rm I} = {}^3/_2$ ${}^1/_2$ $-{}^1/_2$, and $-{}^3/_2$ and linewidths Γ_i (eq 1). According to Anderson's model, in the presence of an unique exchange interaction that couples the copper centers of the lattice, the relaxation function becomes 9,10

$$\varphi(t) = \mathbf{W} \cdot \exp\{[i(\boldsymbol{\omega} + i\boldsymbol{\Gamma}) + \boldsymbol{\pi}]t\} \cdot \mathbf{1}$$
 (4)

where the components of the vector **W** are proportional to the occupation probabilities of the different states of the system (assumed to be equal in Cu(glu)phen), **1** is a vector with all components equal to one, $\boldsymbol{\omega}$ and $\boldsymbol{\Gamma}$ are diagonal matrices whose elements are the absorption frequencies ω_i and linewidths Γ_i in the absence of exchange, respectively, and $\boldsymbol{\pi}$ is a matrix whose elements give the transition probabilities, which are proportional to $\omega_{\rm ex}$ between the resonance lines. The Fourier transform of eq 3 can be solved without explicit diagonalization of the complex matrix $[i(\omega+i\boldsymbol{\Gamma})+\boldsymbol{\pi}]$ in eq 4, to obtain the line shape function $I(\omega)$ of the spectra³⁴

$$I(\omega) = \text{Re}\{\mathbf{W} \cdot [i(\omega - \omega \mathbf{E} + i\Gamma) + \boldsymbol{\pi}]^{-1} \cdot \mathbf{1}\}$$
 (5)

where E is the unit matrix. This equation predicts a unique solution which can be analytically obtained for the cases of two interacting dissimilar $S = \frac{1}{2}$, spins and of dimeric systems coupled by interdimeric exchange interactions, ¹⁴ as π is a 2 × 2 matrix with $-\omega_{\rm ex}$ and $\omega_{\rm ex}$ as the diagonal and off-diagonal elements, respectively. However, in the case we are dealing with, π is a 4 \times 4 matrix that has two extreme possible constructions, as discussed in the Introduction. Case "a" considers equal transition probabilities between the four lines $(-\omega_{\rm ex}$ and $\omega_{\rm ex}/3$ are the diagonal and off-diagonal matrix elements, respectively), whereas in case "b" only transitions between adjacent lines are allowed (the off-diagonal matrix elements are $\omega_{\rm ex}/2$ adjacent to the diagonal ones and zero otherwise; $-\omega_{\rm ex}/2$ and $-\omega_{\rm ex}$ are the outer and inner diagonal matrix elements, respectively). An alternative approach to analyze the narrowing phenomenon comes from the diagonalization of the matrix $[i(\omega - \omega E + i\Gamma) + \pi]$ in eq 4, where the imaginary part of the matrix eigenvalues gives the line position and the real part, the line width. This procedure gives a way of dividing the spectrum into components and can be useful to obtain an estimation of $\omega_{\rm ex}^{35-37}$ but it does not predict the line shape of the spectrum, which can be obtained only by solving eq 5.

For the case of $S={}^1/{}_2$ spin systems coupled to one nucleus with $I \geq 1$, it is simpler to solve eq 5 numerically. Simulations of the spectra with eq 5 in magnetic field units using the position of the resonance lines predicted by the g-tensor of the Cu(II) ions (Figure 5,Table 1) are shown in Figure 4 for cases "a" and "b" (See also Supporting Information). As shown in this figure, the simulations reproduce reasonably well the angular variation of the spectra for both cases but show some slight discrepancies for some magnetic field orientations in the weak exchange region (Figure 5, spectra between 40° and 100°). These differences may be attributed to our assumption of equal both separation and line width for the four hyperfine components, but it may happen that $m_{\rm I}$ -depending line shape and line separation distortions appear, little away from the expected regular copper hyperfine quartet.³⁸

A qualitative inspection of the spectra simulated for case "a" shows that the four lines shift uniformly toward the gravity center as the spectra approach the collapse condition. In contrast, for case "b", spectral angular variation seems to indicate that the two central resonances collapse first and the outer later. It is evident that a comparison between experimental and simulated spectra cannot allow discerning between any of these two possibilities, as the main features of the spectra can be reasonably reproduced under both schemes. However, it is worth to note the different order of magnitude necessary to produce the merging of the hyperfine structure. Whereas for case "a" the exchange frequency ($\hbar\omega_{\rm ex} = 74 \times 10^{-4}$ cm⁻¹) that reproduces the spectra is approximately of the order of the mean hyperfine line separation ($A_{iso} = 73 \times 10^{-4} \text{ cm}^{-1}$), a 5 times higher exchange frequency is needed for case "b" ($\hbar\omega_{\rm ex}$ = 370×10^{-4} cm⁻¹). The latter value is much higher than those expected for systems having $\pi - \pi$ interactions as superexchange chemical paths. ^{13,14,25,27} Hence, spectral simulation assuming case "b" predicts collapse conditions out of realism despite the fact that it may give a qualitative explanation of the exchange narrowing phenomenon.

Exchange Interaction and Superexchange Paths. The exchange interaction in Cu(glu)phen can be ascribed to the chemical paths shown in Figures 1 and 2. On the basis of the structural data, two possible magnetic behaviors may be

speculated. One is that the exchange constant that couples CuA and CuB ions of the same unit cell (I_{AB}) be dominant (Figure 1A), in which case the EPR behavior should mainly correspond to that of a dimer system. Conversely, if the aromatic π -stacking were the dominant superexchange path $(J_{AB'}$ and $J_{AB''}$), spectra should show features associated with 1D magnetic behavior. As none of these behaviors were observed and the line widths could be reasonably fitted using the second moment of the dipolar interaction, it is concluded that the CuA- $O_{ap}H\cdots O-C-O_{eq}$ -CuB and aromatic π -stacking chemical paths present J-values of the same order of magnitude. This is in line with results obtained in the copper mixed complex with aspartic acid and bypiridine. 16 Since each copper ion of the lattice is linked to three neighbors (see Figures 1 and 2), the relation between the exchange frequency and the exchange coupling constants may be assumed to be $\omega_{\rm ex} \approx 3 J/\hbar$, which determines $|J| \approx 25 \times 10^{-4} \text{ cm}^{-1}$.

CONCLUSIONS

EPR measurements on oriented single crystal samples of Cu(glu)phen show how the spectral lines of a hyperfine multiplet are modulated by weak intercenter exchange interactions mediated by noncovalent interactions. The EPR spectra were interpreted using Anderson's model of exchange narrowing to evaluate both the molecular g-tensor of the copper ions and the exchange frequency that couples the nearest neighboring copper centers of the lattice. Numerical simulations of the angular variation of the EPR spectra showed that the collapse of the hyperfine structure of the copper centers is due to an exchange-mediated mechanism that couples each line of the 2I + 1 transitions to all other lines of the spectrum with the same transition probability (case "a"). The exchange interaction responsible for the changes experienced by the multiplet structure of the isolated Cu ions is mediated by the hydrophobic interaction between two phen molecules and a mixed chemical path of the type CuA-O_{ap}H···O-C-O_{eq}-CuB, for which we evaluated $|J| \approx 25 \times 10^{-4} \text{ cm}^{-1}$, in line with I-values found for other compounds having similar superexchange chemical paths. As chemical paths with these characteristics have been proposed to serve as electron transfer pathways in redox metalloproteins, these results may also be useful to give insight on electron transfer processes through long distances.

ASSOCIATED CONTENT

Supporting Information

Elemental analysis, tables containing single crystal diffraction data and selected bond and angles, figures containing EPR spectra obtained in the ab^* and c^*b^* crystal planes, together with numerical spectral simulation of the spectra using the derivative of eq 5, angular variation of the square g-factor at Q-band, angular variation of the square root of the dipolar second moment in three crystal planes, and temperature dependence of powder EPR spectra at X-band. This material is available free of charge via the Internet at http://pubs.acs.org.

AUTHOR INFORMATION

Corresponding Author

*E-mail, brondino@fbcb.unl.edu.ar. Fax: +54-342-4575221. Telephone: +54-342-4575213.

Notes

The authors declare no competing financial interest.

ACKNOWLEDGMENTS

We thank FONCyT, CONICET, and CAI+D-UNL for financial support. We thank the Spanish Research Council (CSIC) for providing a free of charge license to the Cambridge Structural Database.³⁹ N.I.N., V.G.F., and F.M.F. thank CONICET for fellowship grants. C.D.B. is a member of CONICET-Argentina.

REFERENCES

- (1) Boonmak, J.; Youngme, S.; Chaichit, N.; van Albada, G. A.; Reedijk, J. Cryst. Growth Des. 2009, 9, 3318–3326.
- (2) Chen, J. Y. C.; Jayaraj, N.; Jockusch, S.; Ottaviani, M. F.; Ramamurthy, V.; Turro, N. J. J. Am. Chem. Soc. **2008**, 130, 7206–7207.
- (3) Vázquez, M.; Taglietti, A.; Gatteschi, D.; Sorace, L.; Sangregorio, C.; González, A. M.; Maneiro, M.; Pedrido, R. M.; Bermejo, M. R. Chem. Commun. 2003, 9, 1840–1841.
- (4) Bertrand, P.; More, C.; Guigliarelli, B.; Fournel, A.; Bennett, B.; Howes, B. J. Am. Chem. Soc. 1994, 116, 3078–3086.
- (5) Brondino, C. D.; Rivas, M. G.; Romão, M. J.; Moura, J. J. G.; Moura, I. Acc. Chem. Res. **2006**, 39, 788–796.
- (6) Calvo, R.; Isaacson, R. A.; Paddock, M. L.; Abresch, E. C.; Okamura, M. Y.; Maniero, A. L.; Brunel, L. C.; Feher, G. *J. Phys. Chem.* B **2001**, *105*, 4053–4057.
- (7) Hoffmann, S. K.; Hilczer, W.; Goslar, J. Appl. Magn. Reson. 1994, 7, 289-321.
- (8) Calvo, R. Appl. Magn. Reson. 2007, 31, 271-299.
- (9) Anderson, P. W.; Weiss, P. R. Rev. Mod. Phys. 1953, 25, 269–276.
- (10) Anderson, P. W. J. Phys. Soc. Jpn. 1954, 9, 316-339.
- (11) Farach, H. A.; Strother, E. F.; Poole, C. P., Jr J. Phys. Chem. Solids 1970, 31, 1491–1510.
- (12) Hoffmann, S. K. Chem. Phys. Lett. 1983, 98, 329-332.
- (13) Brondino, C. D.; Calvo, R.; Atria, A. M.; Spodine, E.; Nascimento, O. R.; Peña, O. *Inorg. Chem.* **1997**, *36*, 3183–3189.
- (14) Neuman, N. I.; Perec, M.; González, P. J.; Passeggi, M. C. G.; Rizzi, A. C.; Brondino, C. D. J. Phys. Chem. A **2010**, 114, 13069–13075.
- (15) Brondino, C. D.; Casado, N. M. C.; Passeggi, M. C. G.; Calvo, R. Inorg. Chem. 1993, 32, 2078–2084.
- (16) Brondino, C. D.; Calvo, R.; Atria, A. M.; Spodine, E.; Peña, O. *Inorg. Chim. Acta* **1995**, 228, 261–266.
- (17) Calvo, R.; Steren, C. A.; Piro, O. E.; Rojo, T.; Zuniga, F. J.; Castellano, E. E. *Inorg. Chem.* **1993**, 32, 6016–6022.
- (18) Gramaccioli, C. M.; Marsh, R. E. Acta Crystallogr. 1966, 21, 594-600.
- (19) Baggio, R. F.; Calvo, R.; Brondino, C.; Garland, M. T.; Atria, A. M.; Spodine, E. *Acta Crystallogr., Sect. C* **1995**, *51*, 382–385.
- (20) Antolini, L.; Marcotrigiano, G.; Menabue, L.; Pellacani, G. C.; Saladini, M. *Inorg. Chem.* **1982**, *21*, 2263–2267.
- (21) Antolini, L.; Marcotrigiano, G.; Menabue, L.; Pellacani, G. C. Inorg. Chem. 1983, 22, 141–145.
- (22) Antolini, L.; Marcotrigiano, G.; Menabue, L.; Pellacani, G. C.; Saladini, M.; Sola, M. *Inorg. Chem.* **1985**, *24*, 3621–3626.
- (23) Antolini, L.; Battaglia, L. P.; Bonamartini Corradi, A.; Marcotrigiano, G.; Menabue, L.; Pellacani, G. C.; Saladini, M.; Sola, M. *Inorg. Chem.* **1986**, *25*, 2901–2904.
- (24) Biswas, C.; Drew, M. G. B.; Estrader, M.; Ghosh, A. Dalton Trans. 2009, 5015-5022.
- (25) Voronkova, V.; Galeev, R.; Korobchenko, L.; Madalan, A. M.; Andruh, M.; Kravtsov, V. C.; Simonov, Y. A. *Appl. Magn. Reson.* **2005**, 28, 297–310.
- (26) Calvo, R.; Abud, J. E.; Sartoris, R. P.; Santana, R. C. Phys. Rev. B: Condens. Matter Mater. Phys. 2011, 84, 104433-104445.
- (27) Venegas-Yazigi, D.; Brown, K. A.; Vega, A.; Calvo, R.; Aliaga, C.; Santana, R. C.; Cardoso-Gil, R.; Kniep, R.; Schnelle, W.; Spodine, E. *Inorg. Chem.* **2011**, *50*, 11461–11471.
- (28) Sheldrick, G. Acta Crystallogr., Sect. A 2008, 64, 112-122.

- (29) Schveigkardt, J. M.; Rizzi, A. C.; Piro, O. E.; Castellano, E. E.; De Santana, R. C.; Calvo, R.; Brondino, C. D. Eur. J. Inorg. Chem. **2002**, 2913–2919.
- (30) Stoll, S.; Schweiger, A. J. Magn. Reson. 2006, 178, 42-55.
- (31) Hitchman, M. A.; Kwan, L.; Engelhardt, L. M.; White, A. H. J. Chem. Soc., Dalton Trans. 1987, 457–465.
- (32) Abragam, A. The principles of nuclear magnetism; Clarendon Press: Oxford, U.K., 1961.
- (33) Bencini, A., Gatteschi, D. Electron Paramagnetic Resonance of Exchange Coupled Systems; Springer-Verlag: Berlin, Germany, 1990.
- (34) Sack, R. A. Mol. Phys. 1958, 1, 163-167.
- (35) Strother, E. F.; Farach, H. A.; Poole, C. P. Phys. Rev. A 1971, 4, 2079-2087.
- (36) Brondino, C. D.; Calvo, R.; Baran, E. J. Chem. Phys. Lett. 1997, 271, 51-54.
- (37) Rizzi, A. C.; Brondino, C. D.; Calvo, R.; Baggio, R.; Garland, M. T.; Rapp, R. E. *Inorg. Chem.* **2003**, *42*, 4409–4416.
- (38) Weil, J. A., Bolton, J. R. Electron Paramagnetic Resonance, 2nd ed.; John Wiley & Sons: Hoboken, NJ, 2007.
- (39) Allen, F. Acta Crystallogr., Sect. B 2002, 58, 380–388.